

New Hg^{2+} and Cu^{2+} Selective Chromo- and Fluoroionophore Based on a Bichromophoric Azine

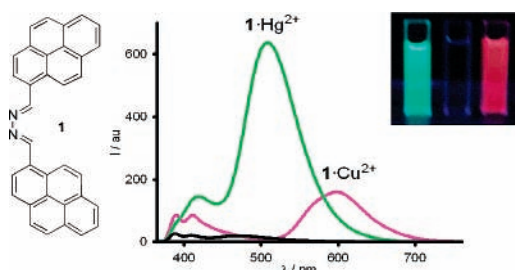
Rosario Martínez, Arturo Espinosa, Alberto Tárraga,* and Pedro Molina*

Departamento de Química Orgánica, Facultad de Química, Universidad de Murcia,
Campus de Espinardo, E-30100 Murcia, Spain

pmolina@um.es

Received October 17, 2005

ABSTRACT



A new probe, 1,4-bis(1-pyrenyl)-2,3-diaza-1,3-butadiene, selectively senses Hg^{2+} and Cu^{2+} through two different channels: the yellow–deep-pink color change and the enhancement of the fluorescence with the red shift of the excimer emission, which can visually be discernible by a green fluorescence in the presence of Hg^{2+} and an orange fluorescence in the presence of Cu^{2+} .

The design and synthesis of fluorescent sensors for heavy and transition-metal ions (HTM) is currently a task of prime importance for environmental or biological applications.¹ Many of the HTM cations are known as fluorescent quenchers via enhancement of spin–orbit coupling (e.g., Hg^{2+})² or energy or electron transfer (e.g., paramagnetic Cu^{2+}).³ The most common fluorescent probes undergo nonspecific quenching with HTM analytes, such as Hg^{2+} and Cu^{2+} . So, the known molecular systems that monitor Hg^{2+} and Cu^{2+} metal ions exploit the mechanism of complexation-induced fluorescence quenching,⁴ and only very few examples for probes

showing a fluorescent enhancement with these metal ions have been reported.⁵

To improve the fluorescence intensity enhancement of the receptor upon binding of Hg^{2+} or Cu^{2+} , one needs to carefully design the receptor molecule containing a fluoro-

(1) (a) de Silva, A. P.; Gunaratne, H. Q. N.; Gunnlaugsson, T.; Huxley, A. J. M.; McCoy, C. P.; Rademacher, J. T.; Rice, T. E. *Chem. Rev.* **1997**, *97*, 1515–1566. (b) *Fluorescent Chemosensors for Ion and Molecule Recognition*; Desvergne, J. P.; Czarnik, A. W., Eds.; Kluwer Academic Publishers: Dordrecht, The Netherlands, 1997. (c) Prodi, L.; Bolletta, F.; Montalti, M.; Zaccaroni, N. *Coord. Chem. Rev.* **2000**, *205*, 59–83. (d) Valeur, B.; Leray, I. *Coord. Chem. Rev.* **2000**, *205*, 3–40. (f) de Silva, A. P.; Fox, D. B.; Huxley, A. J. M.; Moody, T. S. *Coord. Chem. Rev.* **2000**, *205*, 41–57.

(2) McClure, D. S. *J. Chem. Phys.* **1952**, *20*, 682–686.

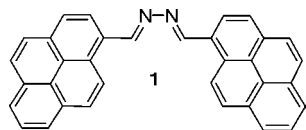
(3) (a) Varnes, A. V.; Dodson, R. B.; Wherry, E. L. *J. Am. Chem. Soc.* **1972**, *94*, 946–950. (b) Kemlo, J. A.; Shepherd, T. M. *Chem. Phys. Lett.* **1977**, *47*, 158–162. (c) Rurack, K.; Resch, V.; Senoner, M.; Dachne, S. *J. Fluoresc.* **1993**, *3*, 141–143.

(4) For mercury: (a) Chae, M.-Y.; Czarnik, A. W. *J. Am. Chem. Soc.* **1992**, *114*, 9704–9705. (b) Rurack, K.; Kollmannsberger, M.; Resch-Genger, U.; Daub, J. *J. Am. Chem. Soc.* **2000**, *122*, 968–969. (c) Prodi, L.; Bargossi, C.; Montalti, M.; Zaccaroni, N.; Su, N.; Bradshaw, J. S.; Izatt, R. M.; Savage, P. B. *J. Am. Chem. Soc.* **2000**, *122*, 6769–6770. (d) Moon, S. Y.; Cha, N. R.; Kim, Y. H.; Chang, S.-K. *J. Org. Chem.* **2004**, *69*, 181–183. (e) Moon, S.-Y.; Youn, N. J.; Park, S. M.; Chang, S.-K. *J. Org. Chem.* **2005**, *70*, 2394–2397. For copper: (a) Sasaki, D. Y.; Shnek, D. R.; Pack, D. W.; Arnold, F. H. *Angew. Chem., Int. Ed. Engl.* **1995**, *34*, 905–907. (b) Torrado, A.; Walkup, G. K.; Imperiali, B. *J. Am. Chem. Soc.* **1998**, *120*, 609–610. (c) Krämer, R. *Angew. Chem., Int. Ed. Engl.* **1998**, *37*, 772–773. (d) Grandini, P.; Mancin, F.; Tecilla, P.; Scrimin, P.; Tonellato, U. *Angew. Chem., Int. Ed.* **1999**, *38*, 3061–3064. (e) Klein, G.; Kaufmann, D.; Schürch, S.; Reymond, J.-L. *Chem. Commun.* **2001**, 561–562. (f) Zheng, Y.; Huo, Q.; Kele, P.; Andreopoulos, F. M.; Pham, S. M.; Leblanc, R. M. *J. Org. Lett.* **2001**, *3*, 3277–3280. (g) Zheng, Y.; Gattás-Asfura, K. M.; Konka, V.; Leblanc, R. M. *Chem. Commun.* **2002**, 2350–2351. (h) Zheng, Y.; Orbulescu, J.; Ji, X.; Andreopoulos, F. M.; Pham, S. M.; Leblanc, R. M. *J. Am. Chem. Soc.* **2003**, *125*, 2680–2686. (i) Boiocchi, M.; Fabbri, L.; Licchelli, M.; Sacchi, D.; Vazquez, M.; Zampa, C. *Chem. Commun.* **2003**, 1812–1813. (j) Roy, B. C.; Chandra, B.; Hromas, D.; Mallik, S. *Org. Lett.* **2003**, *5*, 11–14.

phore so that the responsible mechanism for fluorescence quenching is maximized in the receptor, whereas it is minimized in the metal-bound state of the receptor.

For the selective recognition of soft, heavy metal ions, nitrogen binding sites might be a choice, as is well exemplified with classical azacrown ethers.⁶ Pyrene has often been used as an effective fluorescence probe because of its high detection sensibility.⁷ The emission wavelength of pyrene has been proven to be extremely sensitive to the polarity of the local environment. Formation of the self-assembled complex results in a remarkable change in the fluorescence emission intensities of the pyrene excimer and monomer.⁸ Two informative parameters associated with the pyrene excimer are the intensity ratio of the excimer to the monomer emission (I_E/I_M) and the wavelength corresponding to the maximum of the excimer emission (λ_E). Although the I_E/I_M parameter is sensitive to the structure of the pyrene-labeled systems, the corresponding pyrene λ_E is much less variable and generally locates at 475–485 nm.

On the basis of this body of work, obviously, a suitable designed aza-substituted pyrene derivative might be a good candidate for the selective sensing of HTM ions. This can be realized by combining the 2,3-diazabutadiene group⁹ (azine) as both a putative cation-binding site and a quencher activity with the photoactive behavior of the pyrene ring to endow the signaling properties. In this work, we report the synthesis, characterization, and cation coordination properties of 1,4-bis(1-pyrenyl)-2,3-diaza-1,3-butadiene **1**, in which two photoactive pyrene groups are directly attached by a putative cation-binding site. This small system displays not only the I_E/I_M but also the λ_E variation depending on the metal ion present.



The unreported symmetrical azine **1** was prepared using the one-step reaction between 1-pyrenecarboxaldehyde and

hydrazine hydrate, in 65% yield. The chemosensor behavior with several metal cations (Li^+ , Na^+ , K^+ , Mg^{2+} , Ca^{2+} , Cu^{2+} , Zn^{2+} , Cd^{2+} , Hg^{2+} , Ni^{2+} , Sm^{3+} , Eu^{3+} , Yb^{3+} , and Lu^{3+}) in acetonitrile was investigated by UV/vis and fluorescence measurements, and the titration experiments were analyzed using the computer program Specfit.¹⁰

The absorption spectrum of **1** shows the typical pyrene absorption bands¹¹ in the region 235–391 nm along with a low-energy band centered at 421 nm attributed to the aza bridge, which is responsible for its pale-yellow color. The addition of increasing amounts of Hg^{2+} metal ions to a solution of **1** in acetonitrile ($c = 2.5 \times 10^{-5} \text{ M}$) promotes some changes in its absorption spectrum, with the most significant being the broadening of the absorption bands due to the pyrene ring and the appearance of a new low-energy band at $\lambda = 515 \text{ nm}$. The well-defined isosbestic points at 378 and 460 nm clearly indicate the presence of a unique complex in equilibrium with the free ligand. The new low-energy band, which is red shifted 94 nm, is responsible for the change of color, which is perceptible to the naked eye, from yellowish to a deep-pink (Figure 1). Analysis of

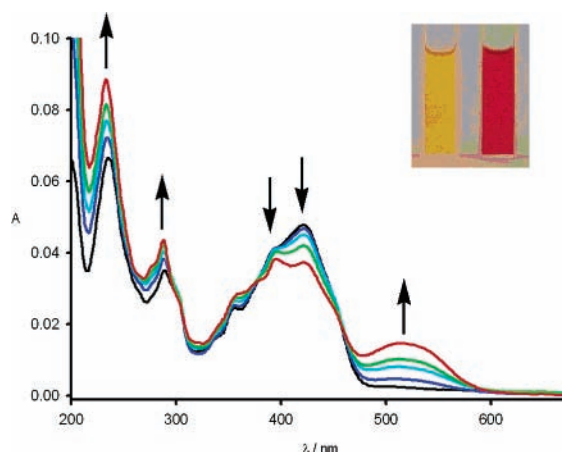


Figure 1. UV/vis spectra obtained during the titration of **1** in CH_3CN ($c = 2.5 \times 10^{-5} \text{ mol dm}^{-3}$) with $\text{Hg}(\text{ClO}_4)_2$. The initial spectrum (black) is that of starting **1**, and the final spectrum (red) corresponds to the complex form $1 \cdot \text{Hg}^{2+}$ after addition of 1 equiv of Hg^{2+} . Arrows indicate the absorptions that increased (up) and decreased (down) during the titration experiments. Inset: Change in the color of **1** after addition of 1 equiv of $\text{Hg}(\text{ClO}_4)_2$. From left to right, in CH_3CN and **1** plus 1 equiv of $\text{Hg}(\text{ClO}_4)_2$ in CH_3CN .

absorption spectral data confirmed a 1:1 ($1/\text{Hg}^{2+}$) binding model and an association constant of $9.70 \times 10^6 \text{ M}^{-1}$.

The Hg^{2+} response of **1** is unaffected in a background of relevant alkali, alkali earth metals, and Group 12 metals Zn^{2+} and Cd^{2+} ; only Cu^{2+} interferes with the Hg^{2+} -induced absorption change. The addition of increasing amounts of Cu^{2+} metal ions to a solution of **1** in acetonitrile promotes the appearance of both a new red shifted low-energy

- (5) For mercury: (a) Nolan, E. M.; Lippard, S. J. *J. Am. Chem. Soc.* **2003**, *125*, 14270–14271. (b) Descalzo, A.; Martínez-Mañez, R.; Radeaglia, R.; Rurack, K.; Soto, J. *J. Am. Chem. Soc.* **2003**, *125*, 3418–3419. (c) Guo, X.; Qian, X.; Jia, L. *J. Am. Chem. Soc.* **2004**, *126*, 2272–2273. (d) Ono, A.; Togashi, H. *Angew. Chem., Int. Ed.* **2004**, *43*, 4300–4302. (e) Hennrich, G.; Sonnenschein, H.; Resch-Genger, U. *J. Am. Chem. Soc.* **1999**, *121*, 5073–5074. (f) Hennrich, G.; Walther, W.; Resch-Genger, U.; Sonnenschein, H. *Inorg. Chem.* **2001**, *40*, 641–644. (g) Zhang, G.; Zhang, D.; Yin, S.; Yang, X.; Shuai, Z.; Zhu, D. *Chem. Commun.* **2005**, 2161–2163. For copper: (a) Chosh, P.; Bharadwaj, P. K. *J. Am. Chem. Soc.* **1996**, *118*, 1553–1554. (b) Ramachandram, B.; Samanta, A. *Chem. Commun.* **1997**, 1037–1038. (c) Rurack, K.; Kollmannsberger, M.; Resch-Genger, U.; Daub, J. *J. Am. Chem. Soc.* **2000**, *122*, 968–969. (d) Yang, J.-S.; Lin, C.-S.; Hwang, C.-Y. *Org. Lett.* **2001**, *3*, 889–892. (e) Wu, Q.; Anslyn, E. *J. Am. Chem. Soc.* **2004**, *126*, 14682–14683. (6) (a) Lehn, J.-M.; Montavon, F. *Helv. Chim. Acta* **1978**, *61*, 67–82. (b) Cha, R. N.; Kim, M. Y.; Kim, Y. H.; Choe, J.-I.; Chang, S.-F. *J. Chem. Soc., Perkin Trans. 2* **2002**, 1193–1196. (c) Rurack, K.; Resch-Genger, U.; Bricks, J. L.; Spies, M. *Chem. Commun.* **2000**, 2103–2104. (7) Winnick, F. M. *Chem. Rev.* **1993**, *93*, 587–614. (8) (a) Nishizawa, S.; Kato, A.; Teramae, N. *J. Am. Chem. Soc.* **1999**, *121*, 9463–9464. (b) Sahoo, D.; Narayanaswami, V.; Kay, C. M.; Ryan, R. O. *Biochemistry* **2000**, *39*, 6594–6601. (9) Son, S. U.; Park, K. H.; Jung, I. G.; Chung, Y. K. *Organometallics* **2002**, *21*, 5366–5372.

(10) Specfit/32 Global Analysis System; Spectrum Software Associates, Claix, France, 1999–2004. (SpecSoft@compuserve.com).

(11) Förster, T.; Kasper, K. Z. *Elektrochem.* **1955**, *59*, 976–980.

absorption band, at $\lambda = 520$ nm ($\Delta\delta = 99$ nm), and two isosbestic points at 361 and 452 nm, clearly indicating the presence of a unique complex in equilibrium with the free ligand (see the Supporting Information). Addition of Cu^{2+} metal ions also showed a naked-eye perceptible color change, from yellowish to a deep-pink. The resulting titration fitted to a 1:1 binding model, and the association constant was $6.9 \times 10^6 \text{ M}^{-1}$.

This behavior is similar to that encountered with several multidentate thioether-containing ligands that exhibit selectivity for metal ions in the “copper triangle” of the Periodic Table.¹²

As expected, ligand **1** showed a very weak fluorescence. The emission spectrum displays typical emission bands at 388 and 409 nm, which are attributed to the pyrene monomeric emission and a red shifted structureless maximum at 475 nm, typical of pyrene excimer fluorescence⁷ ($\lambda_{\text{ex}} = 350$ nm), with a low quantum yield ($\Phi = 0.016$) (see the Supporting Information). The excimer emission band is concentration dependent, which is consistent with intermolecular excimer formation.¹³

Upon addition of small amounts of Hg^{2+} to the solution of ligand **1** in acetonitrile ($c = 2.5 \times 10^{-5} \text{ M}$), a pronounced red shift along with an intensity enhancement of the pyrene excimer emission was observed. An intensity maximum is reached at $[\mathbf{1}]/[\text{Hg}^{2+}] = 1$, where the λ_{E} shifts as much as 33 nm (from 475 to 508 nm) (Figure 2). The final

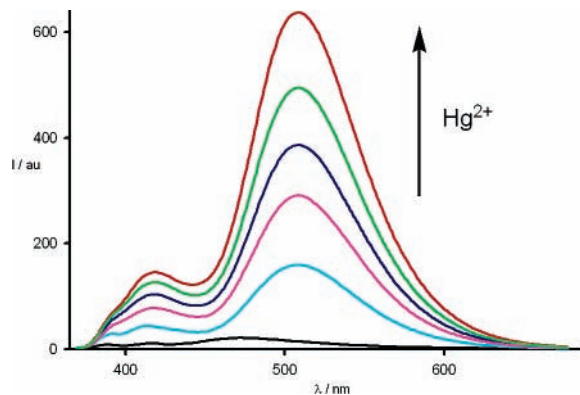


Figure 2. Changes in the fluorescence emission spectra of **1** ($\lambda_{\text{exc}} = 350$ nm) in CH_3CN ($c = 2.5 \times 10^{-5} \text{ mol dm}^{-3}$) upon titration with $\text{Hg}(\text{ClO}_4)_2$ /starting **1** (black) and after addition of 0.2 (cyan), 0.4 (pink), 0.6 (blue), 0.8 (green), and 1 equiv (red) of Hg^{2+} .

fluorescence enhancement factor (FEF) was 30, with the ratio of the fluorescence intensity ($\lambda_{508}/\lambda_{418}$) of the being higher (4.4) than that in the free ligand ($\lambda_{475}/\lambda_{388} = 2.6$), and the quantum yield ($\Phi = 0.17$) resulted in a 10-fold increase compared to that of **1** ($\Phi = 0.016$). The stoichiometry of

the complex system was also determined by the changes in the fluorogenic response of **1** in the presence of varying concentrations of Hg^{2+} , and the results obtained indicate the formation of a 1:1 complex giving an association constant of $1.16 \times 10^6 \text{ M}^{-1}$.

One of the most powerful methods for the differentiation of a dynamic excimer from a static one is the excitation spectrum.⁷ Thus, the excitation spectrum obtained from **1**· Hg^{2+} at the excimer emission ($\lambda = 508$ nm) was different compared with the excitation spectrum taken at the monomer emission wavelength ($\lambda = 418$ nm), which is generally taken as compelling evidence for ground-state preassociation of pyrenes, demonstrating that the emission at $\lambda = 508$ nm corresponds to a static excimer (see the Supporting Information).

Ligand **1** was found to have a detection limit¹⁴ of $3.4 \times 10^{-6} \text{ M}$ as a fluorogenic sensor for the analysis of Hg^{2+} (see the Supporting Information), exhibiting higher sensitivity and selectivity than others previously reported^{5a} although they can operate in pure water.

Quantum chemical calculations at the DFT level (see the Supporting Information) indeed show the preference for a 2:2 complex ($\mathbf{1} \cdot \text{Hg}$)₂⁴⁺ with every Hg atom in a distorted tetrahedral environment made up by one N atom ($d_{\text{N-Hg}} = 2.568 \text{ \AA}$, Wiberg bond index (WBI) = 0.134) and one pyrenyl C-10 atom ($d_{\text{C-Hg}} = 2.457 \text{ \AA}$, WBI 0.273) of every ligand, having overall D_2 symmetry (Figure 3). The latter

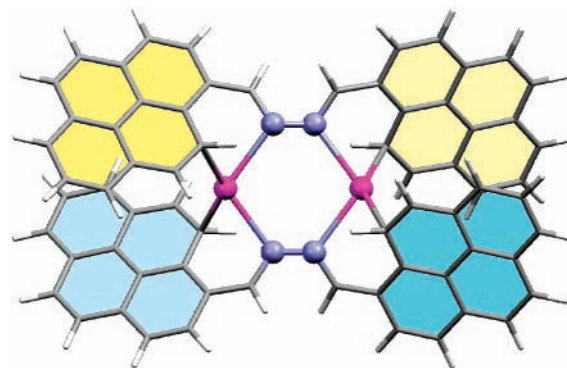


Figure 3. Calculated (B3LYP/6-31G*) structure for the (**1**· Hg)₂⁴⁺ complex.

interaction approaches the two related pyrenyl rings lying almost parallel to each other (angle between mean planes = 24.5°). The resulting six-membered tetraazadimetallacycle has a twisted-boat conformation with a low angle around Hg (107.4°) that keeps both metal atoms far enough to vanish their mutual interaction ($d_{\text{Hg-Hg}} = 4.371 \text{ \AA}$, WBI = 0.002).

As we have mentioned before, addition of Cu^{2+} to ligand **1** does not promote any significant changes in the UV–vis spectrum in comparison with those observed when Hg^{2+} was added. However, the emission spectrum was found to be

(12) Cooper, T. H.; Mayer, M. J.; Leung, K.-H.; Ochrymowycz, L. A.; Rorabacher, D. B. *Inorg. Chem.* **1992**, *31*, 3796–3804 and references therein.

(13) (a) Parker, D.; Williams, J. A. G. *J. Chem. Soc., Perkin Trans. 2* **1995**, 1305–1314. (b) Beeby, A.; Parker, D.; Williams, J. A. G. *J. Chem. Soc., Perkin Trans. 2* **1996**, 1565–1579.

(14) Shortreed, M.; Kopelman, R.; Kuhn, M.; Hoyland, B. *Anal. Chem.* **1996**, *68*, 1414–1418.

strongly dependent on the nature of the metal ion: Cu^{2+} or Hg^{2+} . Moreover, the fluorescence behavior of this ligand in the presence of Cu^{2+} metal ions also depends on the amount of metal ion added. Thus, addition of $0 < n \leq 0.5$ equiv of $\text{Cu}(\text{OTf})_2$ promotes a remarkable red shift above 135 nm of the excimer emission (from $\lambda = 475$ nm to $\lambda = 610$ nm) with concomitant enhancement of the fluorescence intensity, and consequently, the ratio of fluorescence intensity ($\lambda_{610}/\lambda_{388}$) of the excimer/monomer was slightly higher (3.4) than that in the free ligand ($\lambda_{475}/\lambda_{388} = 2.6$). Surprisingly, when $0.5 < n \leq 1$ equiv of Cu^{2+} was added, a slight blue shift along with an enhancement of the pyrene excimer and monomer emissions was observed reaching the maximum intensity enhancement at $[\mathbf{1}]/[\text{Cu}^{2+}] = 1$, where the λ_{E} shifts 20 nm (from 610 to 590 nm) and the ratio of fluorescence intensity of the excimer/monomer ($\lambda_{590}/\lambda_{388}$) was lower (2.1) than that in the free ligand (Figure 4). The FEF was 8 and

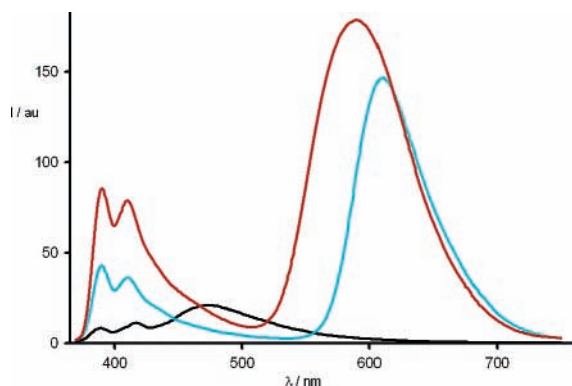


Figure 4. Changes in the fluorescence emission spectra of **1** ($\lambda_{\text{exc}} = 350$ nm) in CH_3CN ($c = 2.5 \times 10^{-5}$ mol dm^{-3}) upon titration with $\text{Cu}(\text{OTf})_2$ /starting **1** (black) and after addition of 0.5 (blue) and 1 equiv (red) of Cu^{2+} .

the quantum yield ($\Phi = 0.033$) was 2-fold larger than that of the free ligand **1** ($\Phi = 0.016$). Titration experiments of the ligand **1** and Cu^{2+} confirmed the empirical 1:1 stoichiometry and gave a value of $5.33 \times 10^6 \text{ M}^{-1}$ for the association constant.

In connection with the above-mentioned considerations about differentiation of a dynamic excimer from a static one, the excitation spectra obtained from $\mathbf{1} \cdot \text{Cu}^{2+}$ at both the excimer emission and the monomer emission wavelengths were also examined, demonstrating that the emission at $\lambda = 590$ nm also corresponds to a static excimer (see the

Supporting Information). In addition, the detection limit, in this case, equaled approximately 3.21×10^{-6} (see the Supporting Information), which is in the range of that exhibited by other sensors detecting Cu^{2+} .^{4h,4i,15}

The calculated structure for the 2:2 D_2 complex $(\mathbf{1} \cdot \text{Cu})_2^{4+}$ (see the Supporting Information) resembles that of mercury but displays a remarkably higher order metal–metal contact ($d_{\text{Cu}-\text{Cu}} = 2.363 \text{ \AA}$, WBI = 0.138) at the expense of negligible interaction with the pyrenyl rings ($d_{\text{C}-\text{Cu}} = 3.167 \text{ \AA}$, WBI = 0.028) that remain less parallel (mean-planes angle = 57.2°). The Cu–Cu bond is favored by an almost flattened six-membered dimetallacycle with a high angle around the coordinatively unsaturated Cu atoms (150.2°).

The fluorescent behavior of ligand **1** provides a good example for distinguishing between Hg^{2+} and Cu^{2+} on the basis of the relative red shift of the excimer emission, notwithstanding the fact that both are intrinsically quenching ions. This red shift can be visually discernible by a green fluorescence in the presence of Hg^{2+} and an orange fluorescence in the presence of Cu^{2+} .

In conclusion, we have devised a new chromo- and fluorogenic ionophore for Hg^{2+} and Cu^{2+} by conjugating a well-known cation-binding unit of 2,3-diaza-1,3-butadiene and an efficient signaling handle of pyrene. The prepared ionophore shows detection limits which are sufficiently low to allow fluorogenic detection of submillimolar concentrations of Hg^{2+} and Cu^{2+} , and it operates through absorption and emission channels: (i) the yellow–deep-pink color change and (ii) enhancement of the fluorescence with the selective red shift of the excimer emission band, which make possible that these two metal ions can be distinguished even visually.

Acknowledgment. We gratefully acknowledge the grants from DGI-Spain CTQ 2004-02201 and Fundación Séneca (CARM-Spain) PB/72/FS/02. R.M. also thanks Ministerio de Educación y Ciencia for a predoctoral grant.

Supporting Information Available: General comments. Relevant spectral and characterization data. UV/vis and fluorescence spectra upon titration with Hg^{2+} and Cu^{2+} . Semilogarithmic plot for determining the detection limits. Figure with the calculated structure for the Cu^{2+} complex and Cartesian coordinates for both complexes. This material is available free of charge via the Internet at <http://pubs.acs.org>.

OL052508I

(15) Our detection limit is also near the range of the values established by the California Department of Health Services for detection of Cu^{2+} in water ($50 \mu\text{g/L}$).